

The HERSCHEL prestellar core population in the Aquila Rift Complex



Initial results from the Gould Belt survey



Vera Könyves
SAP, CEA/Saclay, France

**Ph. André, A. Men'shchikov, N. Schneider,
D. Arzoumanian, S. Bontemps, M. Attard,
F. Motte, P. Didelon, A. Maury**

SPIRE SAG 3 consortium:

**A. Abergel, J.-P. Baluteau, J.-Ph. Bernard, L. Cambrésy,
P. Cox, J. Di Francesco, A.-M. di Giorgio, M. Griffin,
P. Hargrave, M. Huang, J. Kirk, J. Z. Li, P. Martin,
V. Minier, S. Molinari, G. Olofsson, S. Pezzuto, H. Roussel,
D. Russeil, P. Saraceno, M. Sauvage, B. Sibthorpe,
L. Spinoglio, L. Testi, D. Ward-Thompson, G. White,
C. D. Wilson, A. Woodcraft, and A. Zavagno**

Probing the origin of the stellar initial mass function: A wide-field Herschel photometric survey of nearby star-forming cloud complexes

<http://gouldbelt-herschel.cea.fr/>

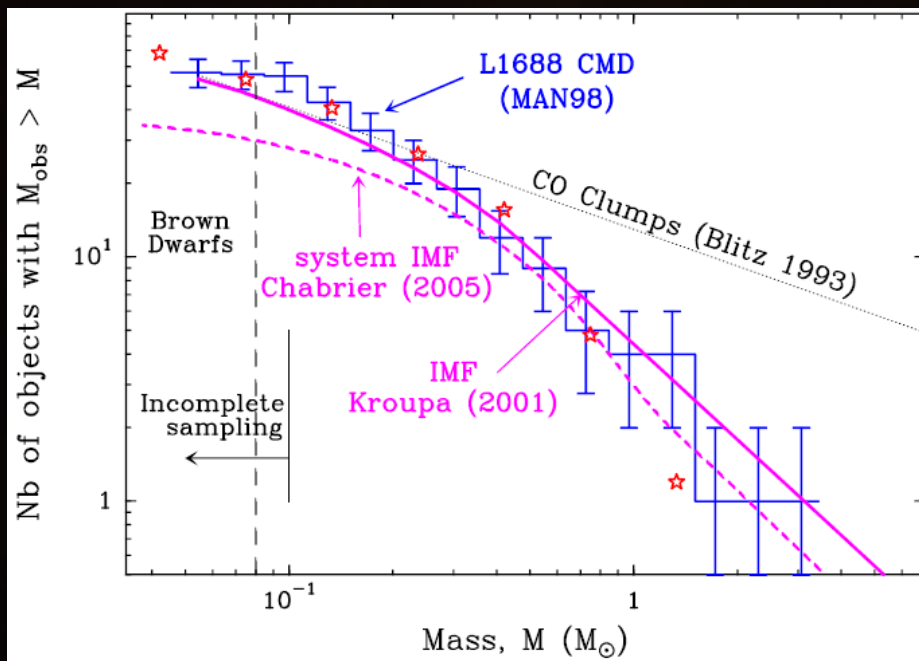
Scientific motivations

- What determines the distribution of stellar masses at birth (IMF)? **What is the link between the prestellar CMF and the stellar IMF?**
- What generates prestellar cores in molecular clouds and governs their evolution to protostars?
- Is core/star formation generally a slow, quasi-static, or a fast, dynamic process?

Ground-based **(sub)-millimeter dust continuum surveys** of nearby, compact cluster-forming clouds (e.g. ρ Ophiuchi, Serpens, Orion B):

- Give 'complete' but small samples of prestellar cores
- Their associated **core mass functions (CMF) resemble the stellar IMF**

E.g.: Motte et al. 1998; Testi & Sargent 1998;
Johnstone et al. 2000; Stanke et al. 2006;
Enoch et al. 2006; Nutter & Ward-Thompson 2007;
Alves et al. 2007; André et al. 2007.



Cumulative mass distribution of 57 starless condensations in ρ Oph (André et al. 2007)

Favored theoretical scenario: **The IMF of solar-type stars is largely determined by pre-collapse cloud fragmentation** (Padoan & Nordlund 2002; Hennebelle & Chabrier 2008).

SDP Observations

SPIRE/PACS parallel-mode observations of the Aquila Rift complex:

- Observed on 24 October 2009
- A common $\sim 11 \text{ deg}^2$ area was covered by both SPIRE/PACS
- Scan maps were taken with $60'' \text{sec}^{-1}$ scanning speed

Data reduction

SPIRE (250/350/500 μm):

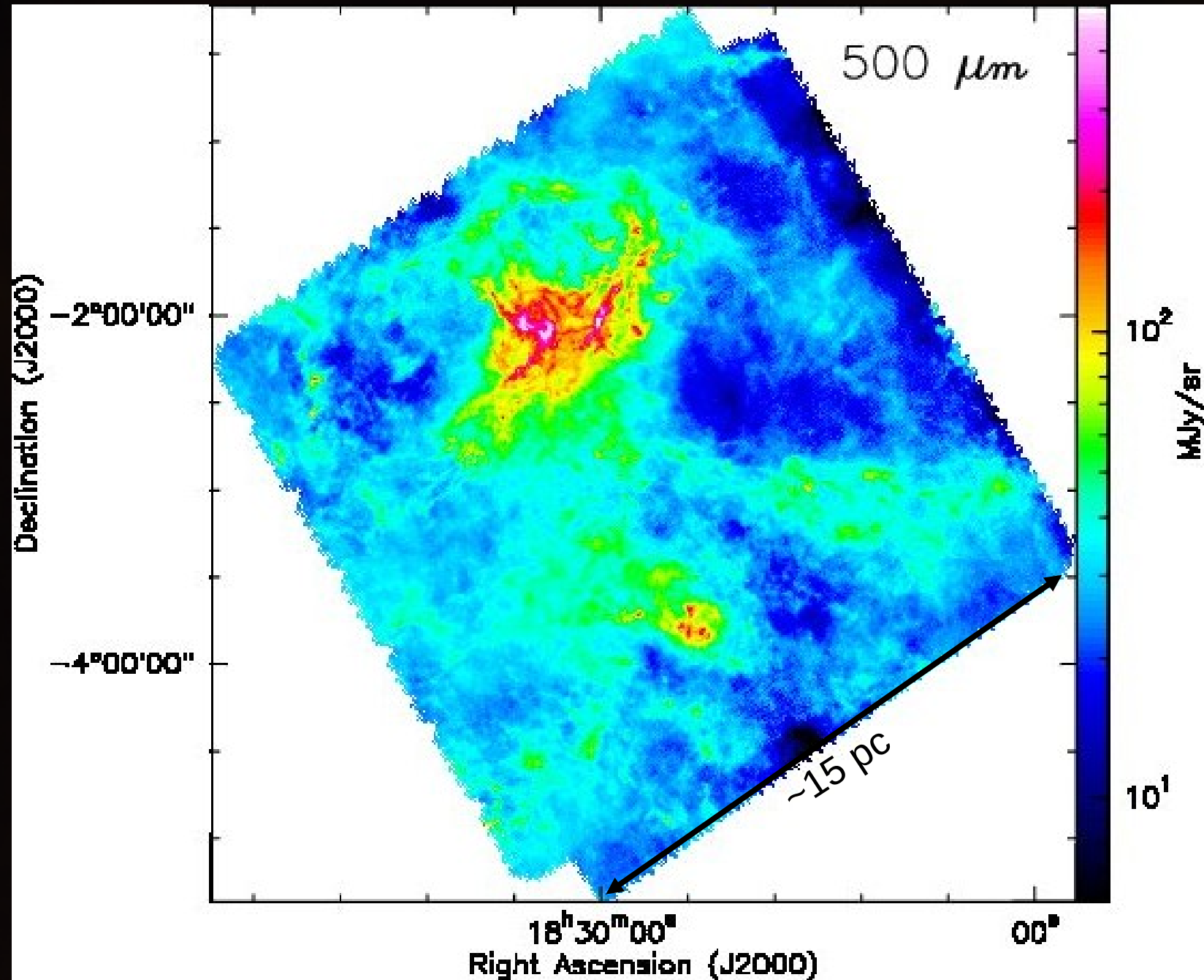
- Using HIPE version 2.0 with modified pipeline scripts, delivered with this version.
- Map making with 'naive' method.

PACS (70/160 μm):

- With HIPE version 3.0, applying standard steps of the default pipeline with modifications.
- Map making with photProject task (later on with madMap).
- *Many thanks to M. Sauvage, B. Ali, H. Aussel, N. Billot, B. Altieri, P. Chaniai, ...*

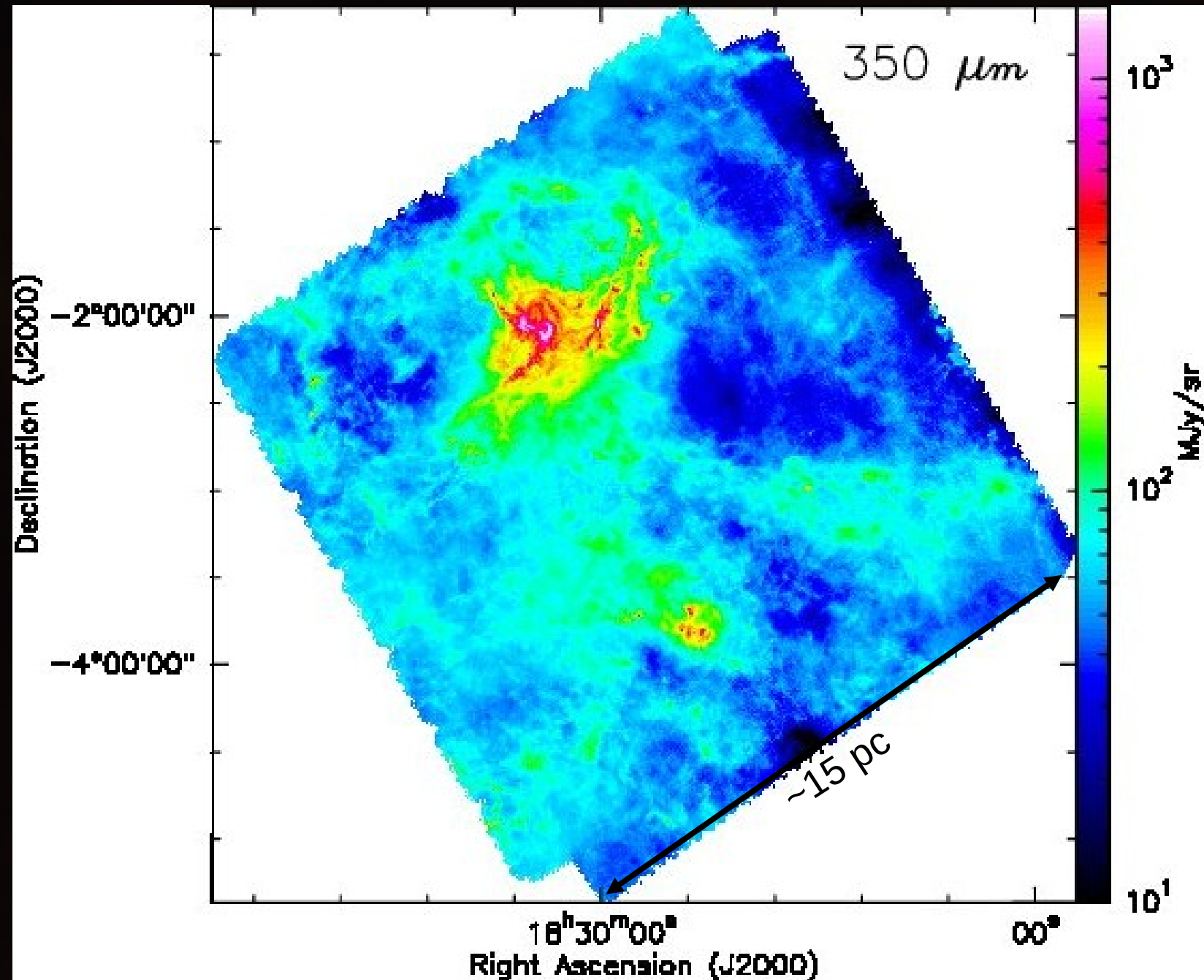
PRESTELLAR CORES IN AQUILA

SPIRE MAPS



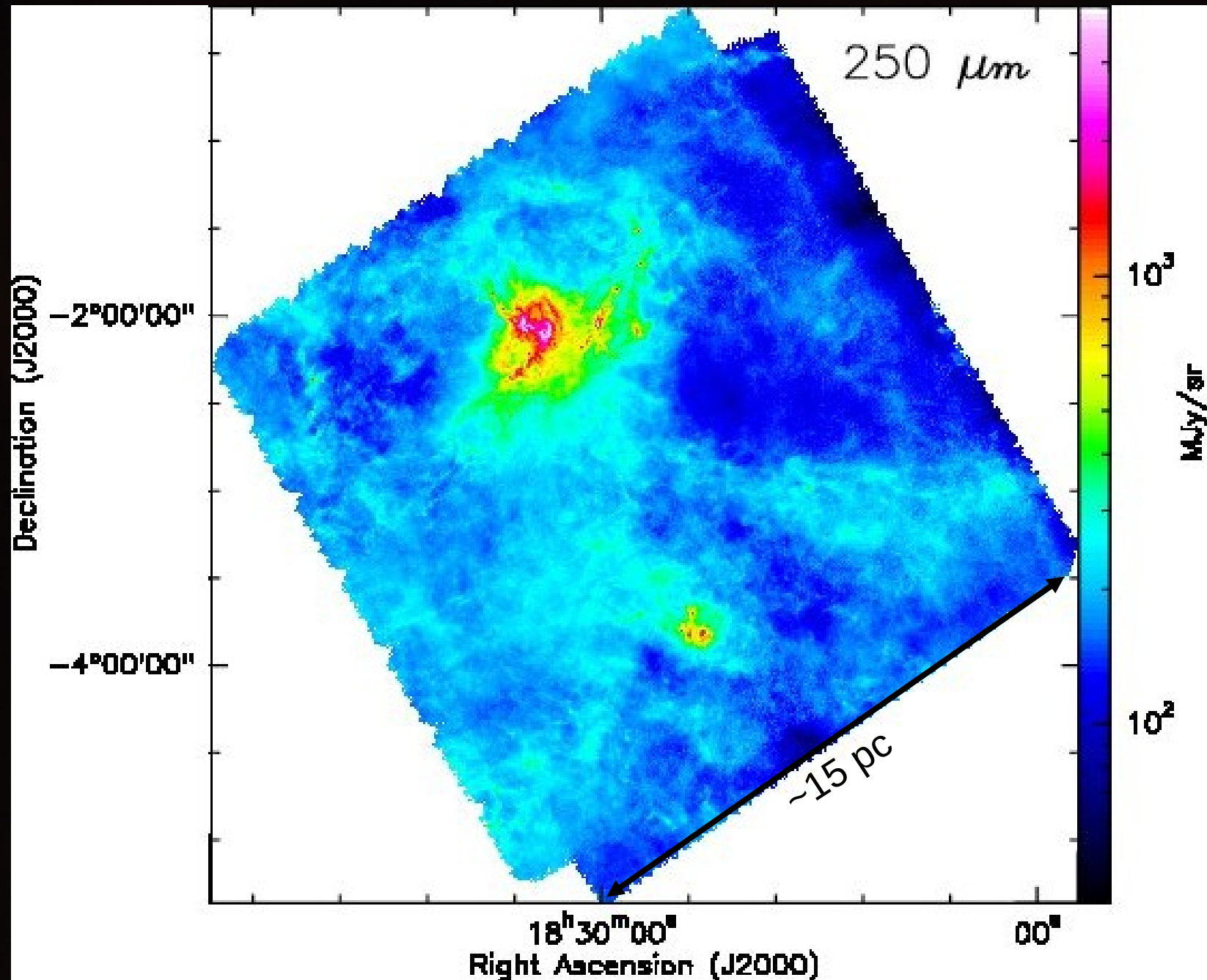
PRESTELLAR CORES IN AQUILA

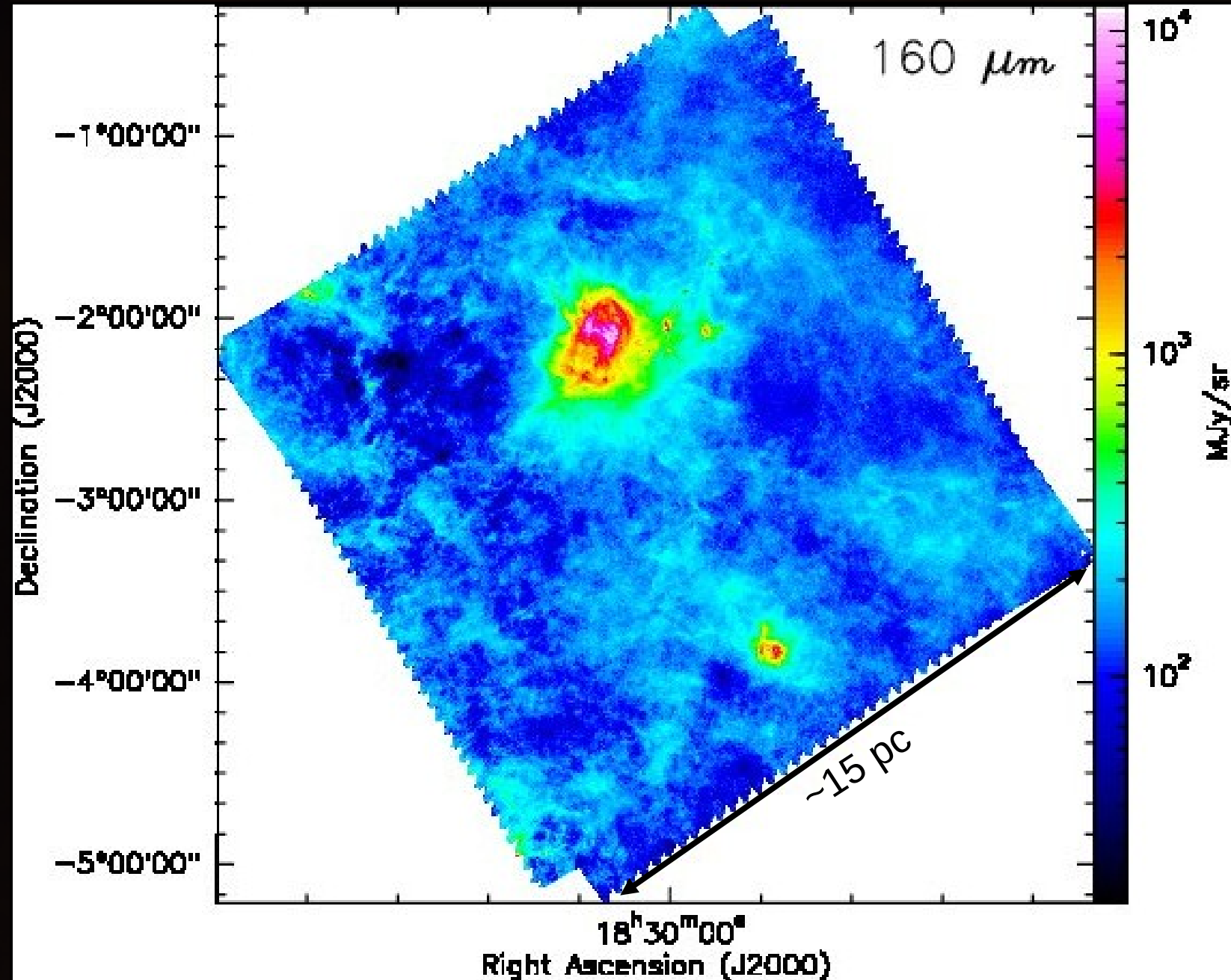
SPIRE MAPS



PRESTELLAR CORES IN AQUILA

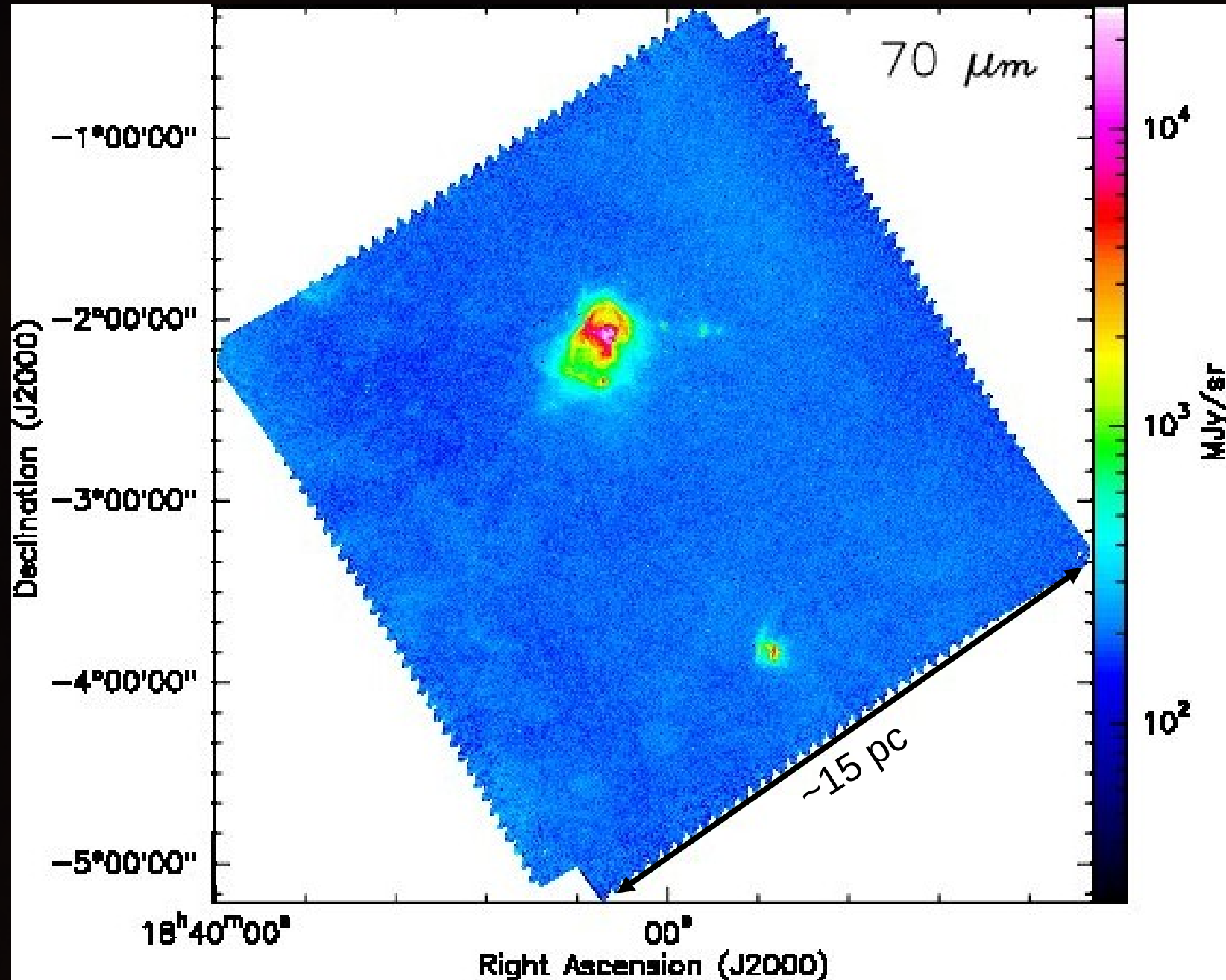
SPIRE MAPS





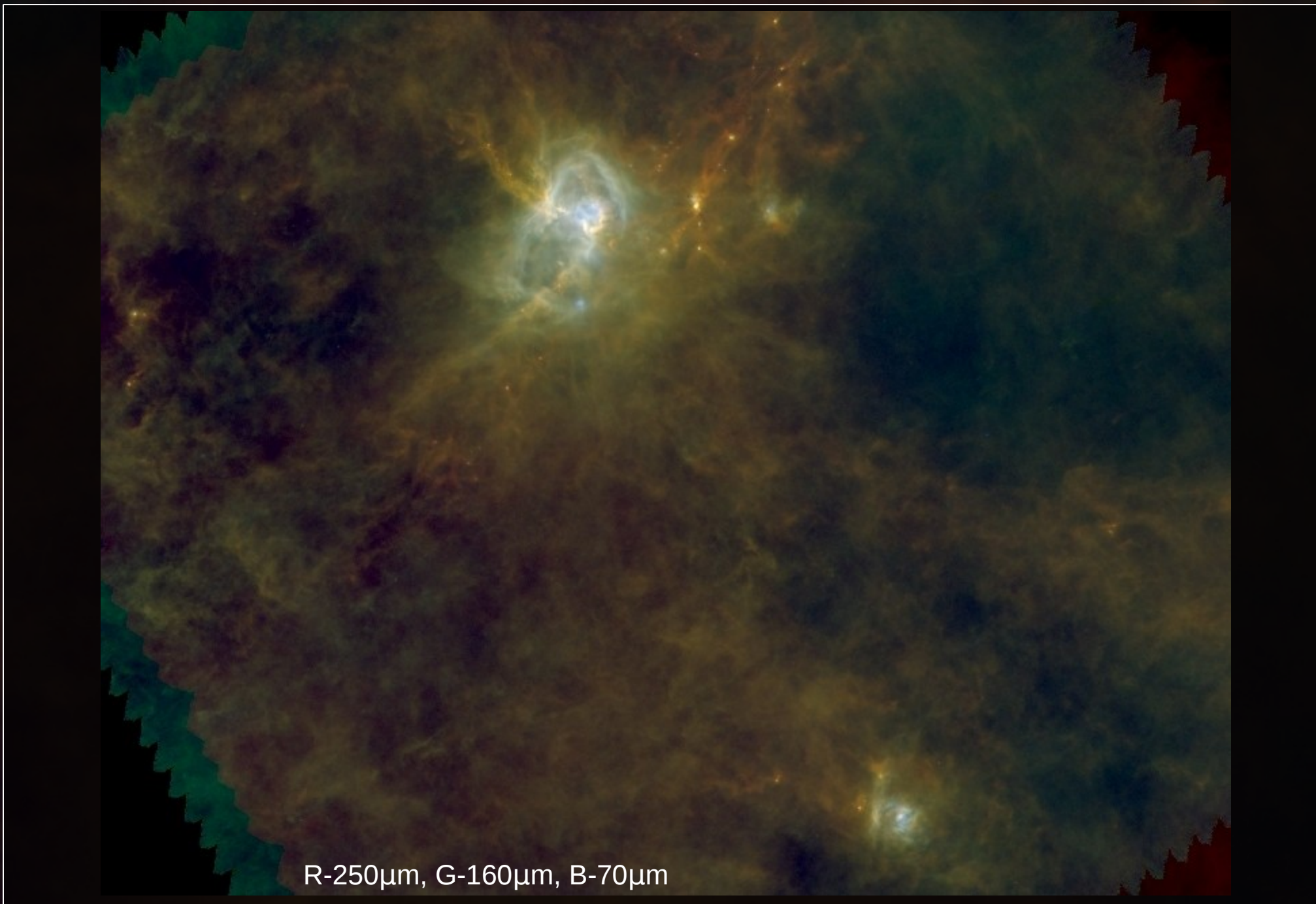
PRESTELLAR CORES IN AQUILA

PACS MAPS



PRESTELLAR CORES IN AQUILA

RGB COMPOSITE IMAGE



R-250 μ m, G-160 μ m, B-70 μ m

Dust temperature (T_d) and column density (Σ) maps, constructed from HERSCHEL SPIRE/PACS data:

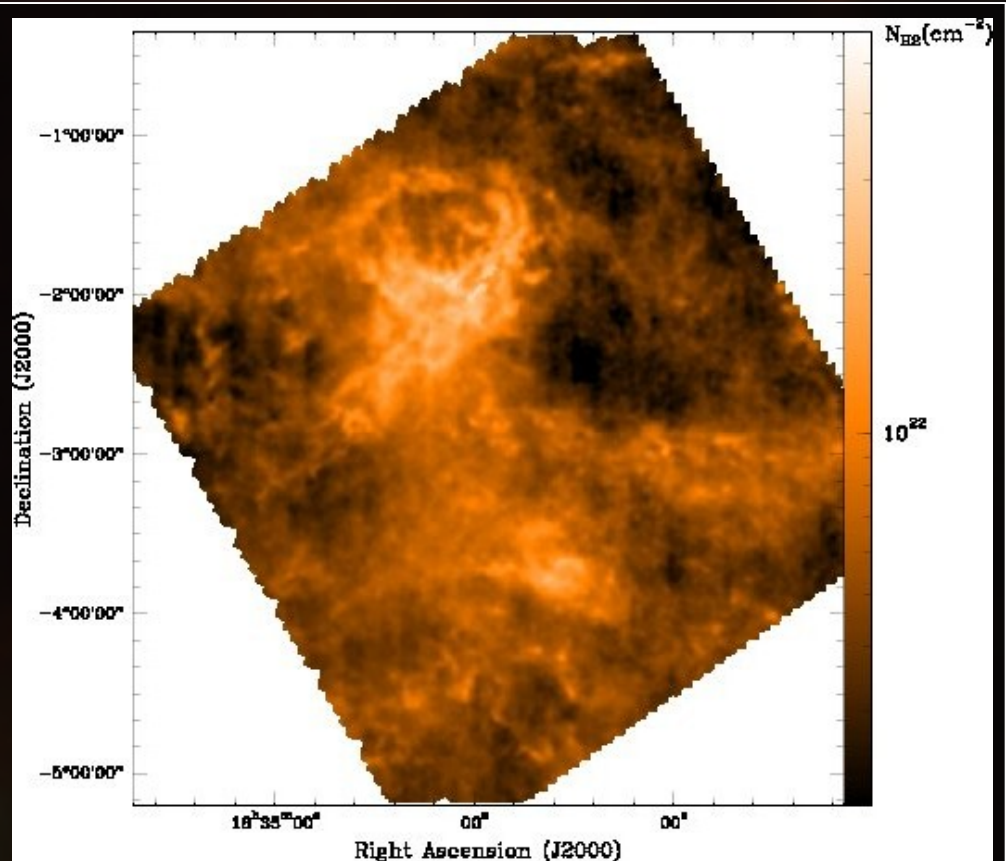
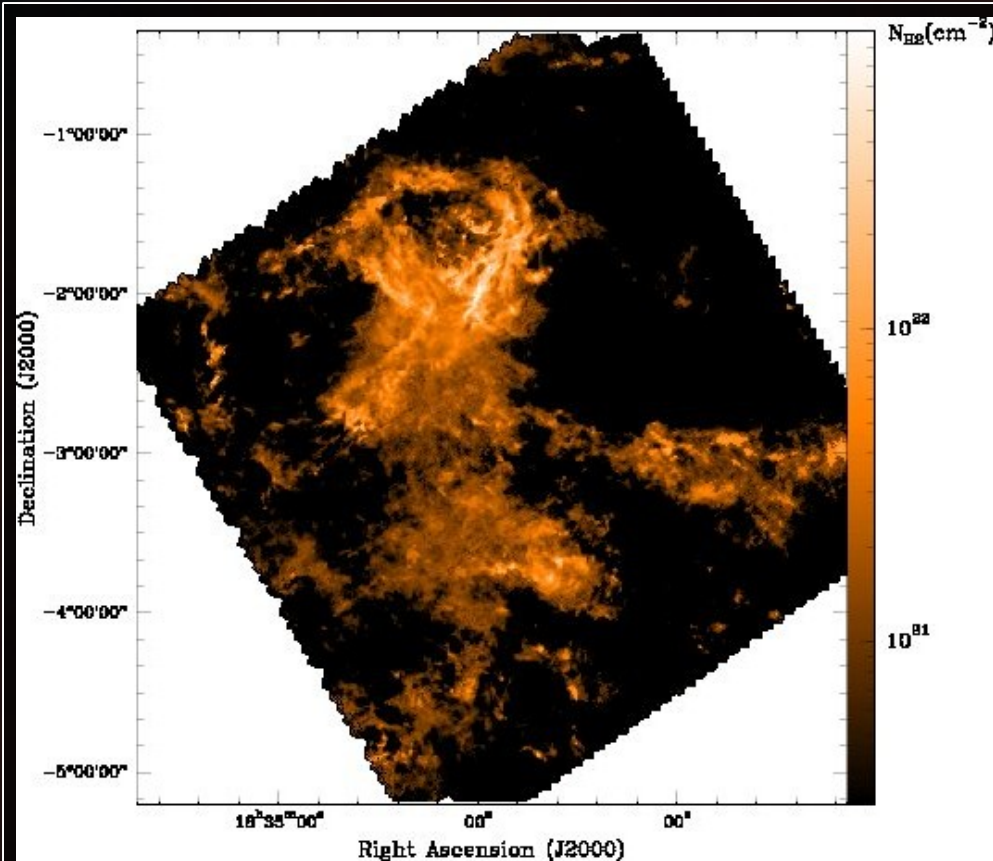
- **Weighted SEDs** constructed for all map pixels from the 5 SPIRE/PACS wavelengths.
- SEDs **fitted by a greybody**, $I_\nu = B_\nu(T_d)(1 - e^{-\tau_\nu})$
 I_ν : observed surface brightness at ν ; $\tau_\nu = \kappa_\nu \Sigma$: dust optical depth; κ_ν : dust opacity per unit (dust+gas) mass, $\beta = 2$ (e.g. Hildebrand 1983).
- The **two free parameters T_d and Σ were derived from the greybody fit** to the 5 Herschel data points for all pixels.

Estimation of dust temperature, column density, and mass of cores:

- A similar SED fitting procedure (above) was employed.
- These **SEDs were constructed from integrated flux densities** measured by `getsources` (Men'shchikov et al. 2010) for the extracted sources.
- **Core mass calculation** using 260 pc to Aquila (see discussion on distance uncertainty in Bontemps et al. 2010; André et al. 2010), estimated **mass uncertainty is a factor of ~ 2** , mainly due to κ_ν .

PRESTELLAR CORES IN AQUILA

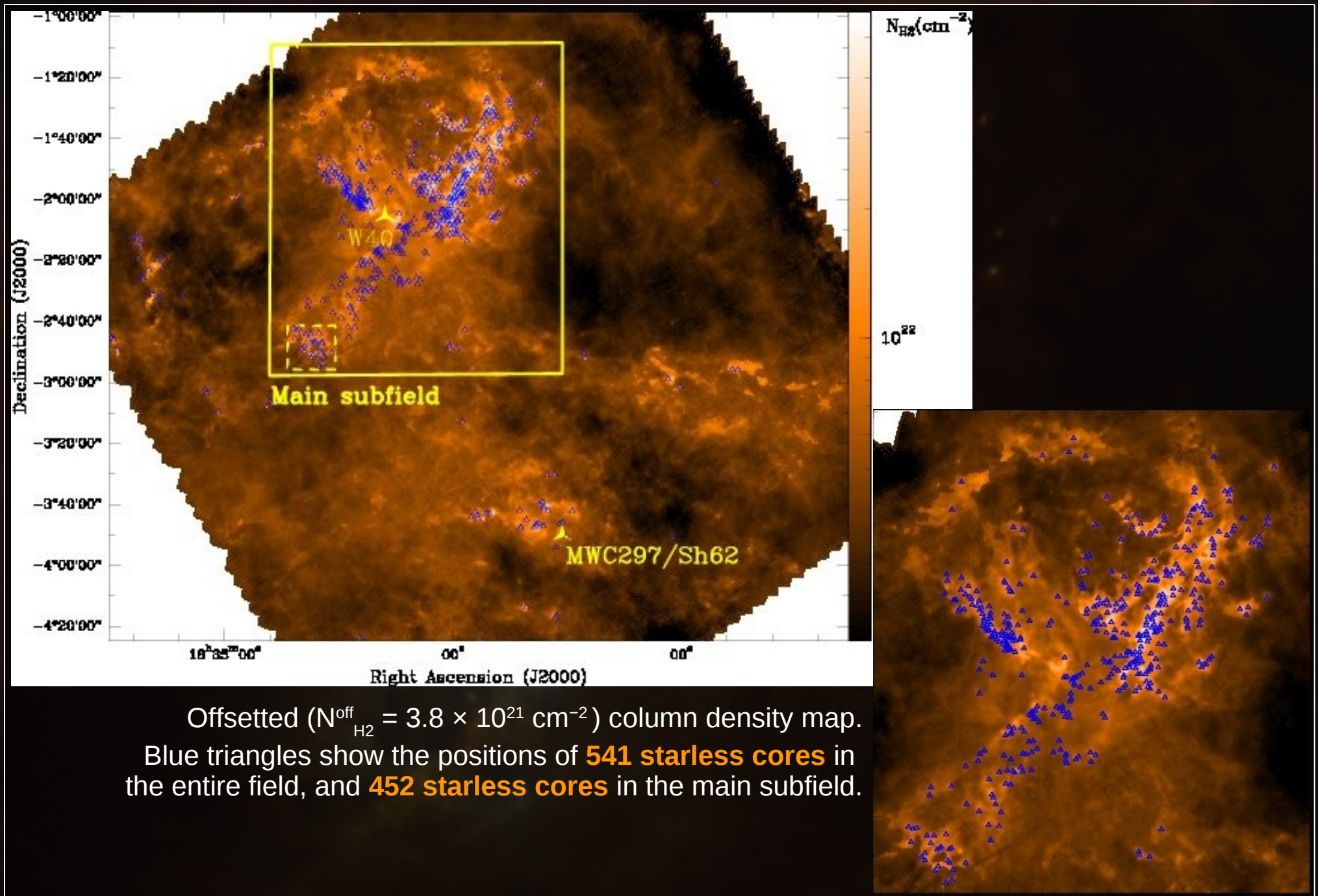
COLUMN DENSITY MAPS



Column density map of the Aquila entire field derived from Herschel data. (FWHM = 36").

Near-IR extinction map based on 2MASS data (Bontemps et al. 2010), in units of column density, using the relation $N_{\text{H}_2} = 10^{21} \text{ cm}^{-2} \times A_V$ (FWHM = 2').

Herschel mapping does not constrain the zero level of the background emission, so **we added a uniform offset $N_{\text{H}_2}^{\text{off}} = 3.8 \times 10^{21} \text{ cm}^{-2}$ to our column density maps** to optimize the match with the near-IR extinction map.



Source extraction

Compact sources were extracted from the SPIRE/PACS images **using getsources**, a multi-scale, multi-wavelength source finding algorithm (Men'shchikov et al. 2010).

Only **robust sources were considered** with significant ($S/N > 7.5$) detections in at least two SPIRE bands.

Distinction between starless cores and protostars/YSOs

Aquila main subfield: Spitzer 24 μm observations + PACS 70 μm data.

- **YSOs:** Detected in emission above the 5σ level at 70 μm and/or 24 μm
- **Starless cores:** undetected in emission (or detected in absorption) at both 70 μm and 24 μm .

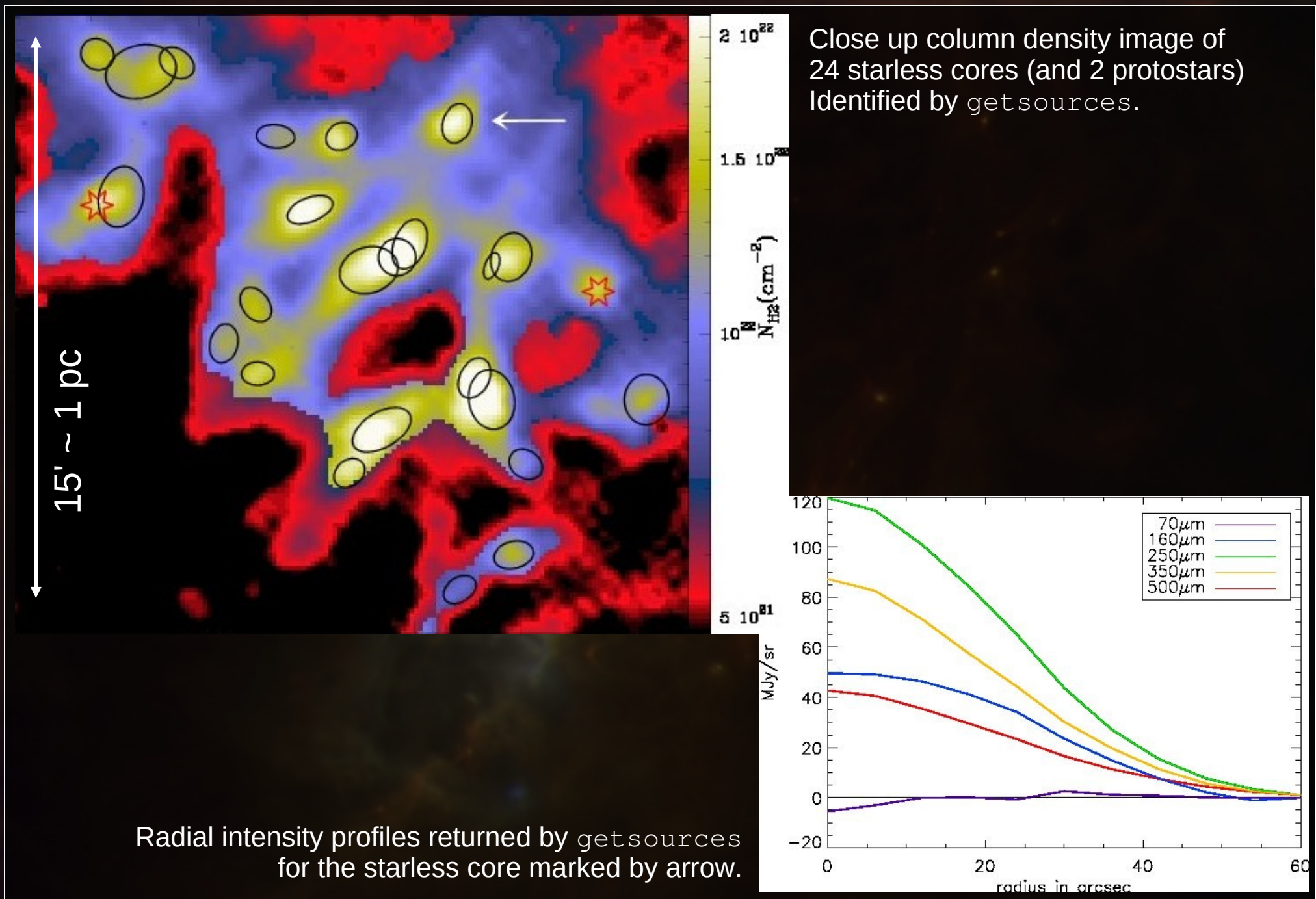
=> 452 starless cores in the Aquila main subfield.

Aquila entire field: Only PACS 70 μm data

=> we identified a total of 541 starless cores and ~170 embedded YSOs (~50 Class 0 protostars, Bontemps et al. 2010).

PRESTELLAR CORES IN AQUILA

CLOSE UP VIEW OF EXTRACTED SOURCES



PRESTELLAR CORES IN AQUILA

PRESTELLAR NATURE OF THE STARLESS CORES I

(I.) We used the **critical Bonnor-Ebert (BE) mass**, $M_{\text{BE}}^{\text{crit}} \approx 2.4 R_{\text{BE}} a^2/G$, as a surrogate for the virial mass, to **determine if the cores are gravitationally bound or not**. R_{BE} : BE radius; a : isothermal sound speed; G : gravitational constant.

Assumptions: thermal motions are dominant over non-thermal motions in starless cores (André et al. 2007)

Then, **two estimates of the BE mass** were derived for each objects:

(1) $M_{\text{BE}}(R_{\text{obs}})$

(2) $M_{\text{BE}}(\Sigma_{\text{cl}})$, where Σ_{cl} is the column density of the local background cloud

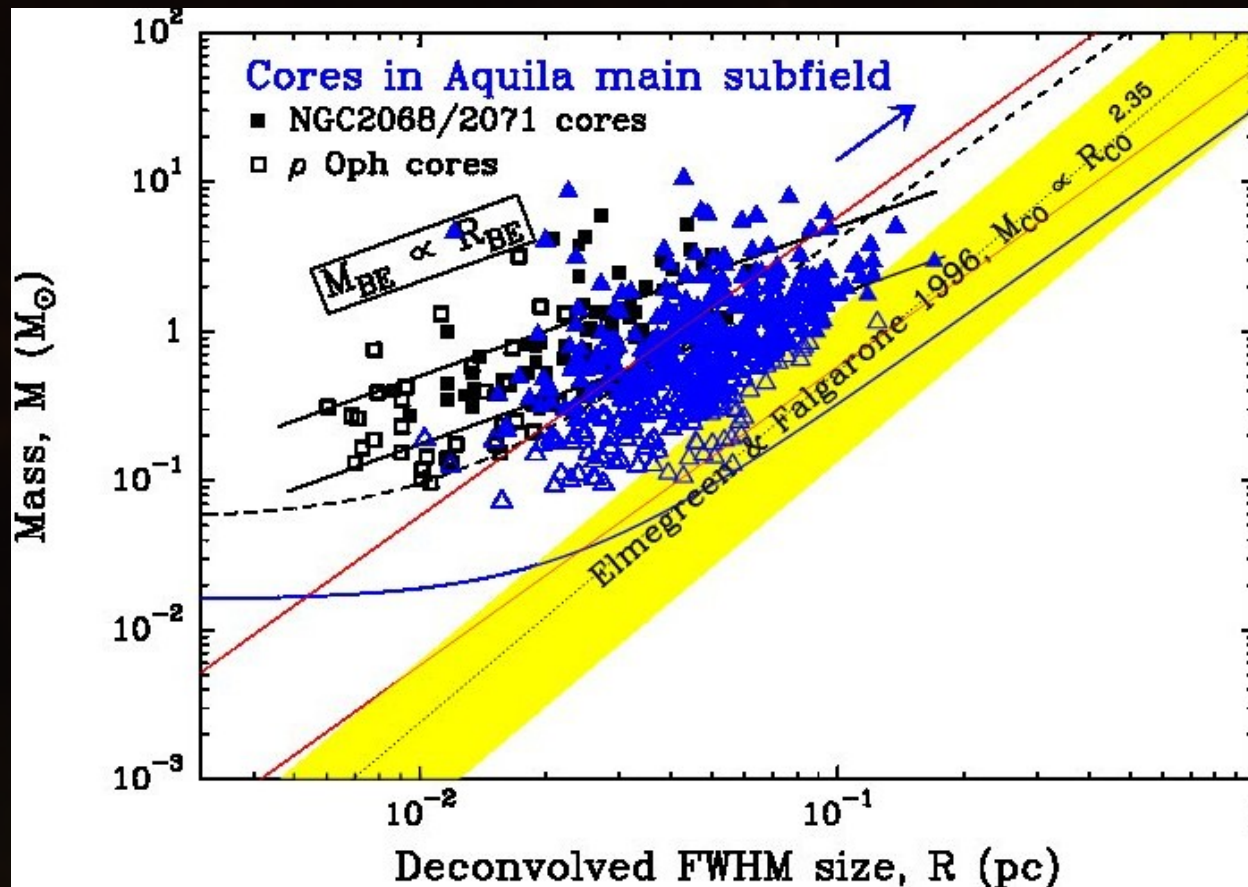
Good candidate prestellar cores, selected from starless cores if their BE mass ratio:

$$\alpha_{\text{BE}} \equiv \max[M_{\text{BE}}(R_{\text{obs}}), M_{\text{BE}}(\Sigma_{\text{cl}})] / M_{\text{obs}} \leq 2.$$

=> ~70 % of the 452 starless cores in the main subfield,

and **more than 60 %** of the 541 starless cores in the entire field **were found to be gravitationally bound**.

(II.) The high fractions of bound objects are consistent with the locations of the Aquila starless cores in a mass vs. size diagram.



Mass vs. size diagram comparing the locations of 314 candidate prestellar cores (\blacktriangle), and the rest starless cores (\triangle), identified with Herschel in the Aquila main subfield, to both models of critical isothermal BE spheres (at $T=7K$ and $T=20K$) and observed prestellar cores (Motte et al. 1998, 2001).

PRESTELLAR CORES IN AQUILA

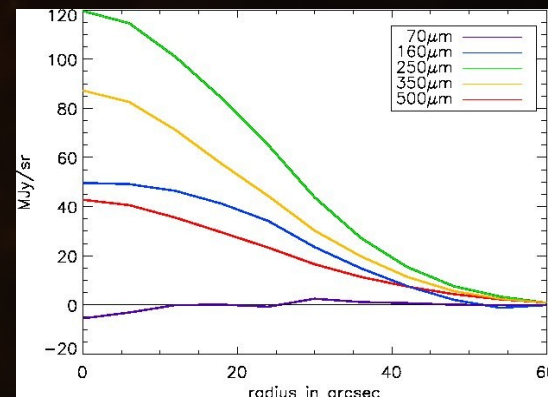
PRESTELLAR NATURE OF THE STARLESS CORES III

(III.) The **self-gravitating character** of most Herschel cores in Aquila is supported **by their internal column density contrast**: $\Sigma_{\text{peak}} / \langle \Sigma_{\text{core}} \rangle$ (peak and mean column densities of the core).

With some assumptions, this can be **estimated from the core intensity values** in the same form: $I_{\nu}^{\text{peak}} / \langle I_{\nu} \rangle$ (peak and mean intensities of the core).

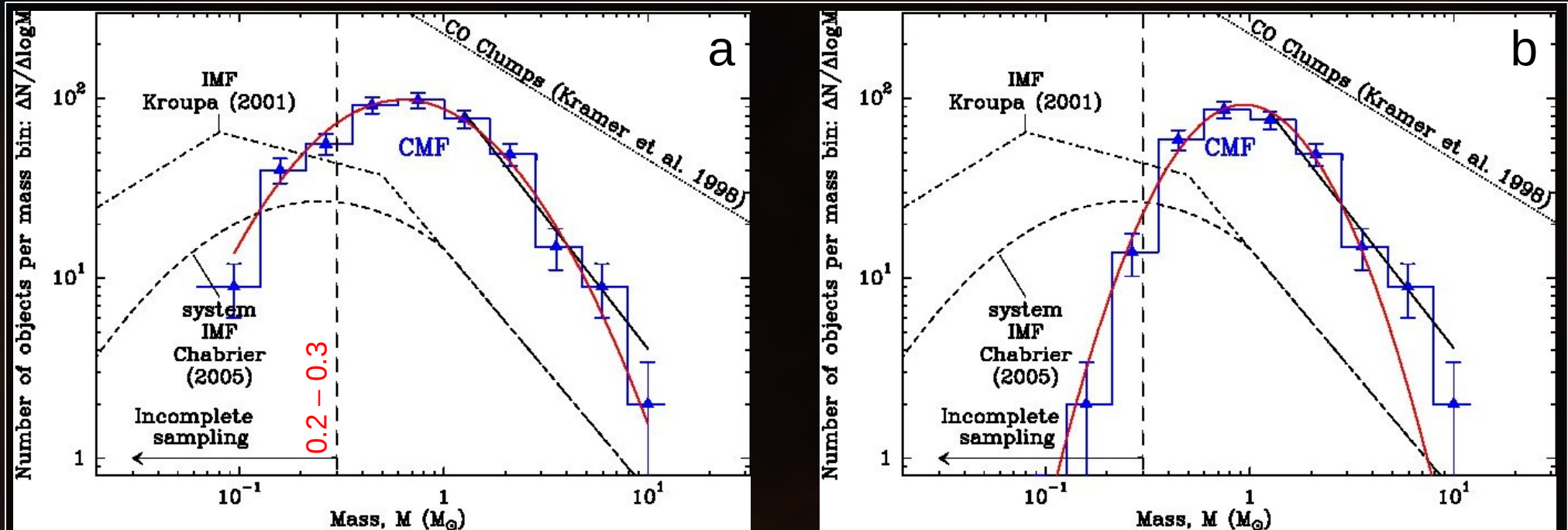
According to theory: $\Sigma_{\text{peak}} / \langle \Sigma_{\text{core}} \rangle > 3.6$ for supercritical self-gravitating BE spheres (Johnstone et al. 2000).

=> Based on their radial intensity profiles, our Aquila starless cores have a median **internal column density contrast** ~ 4 .



(IV.) **Column density contrast of the Herschel cores over the local background**:

=> This test also confirms that **most of the starless cores are self-gravitating, and prestellar in nature**.



Differential mass function of 452 starless cores (a), and of 314 candidate prestellar cores (b) identified in the Aquila main subfield. The mass function is approximated with a lognormal fit, the high-mass end is fitted by a power-law.

(a) Lognormal fit: peak at $\sim 0.6 M_{\odot}$, standard deviation ~ 0.42 in $\log_{10} M$.

fitted power-law: $dN/d\log M \propto M^{-1.5 \pm 0.2}$

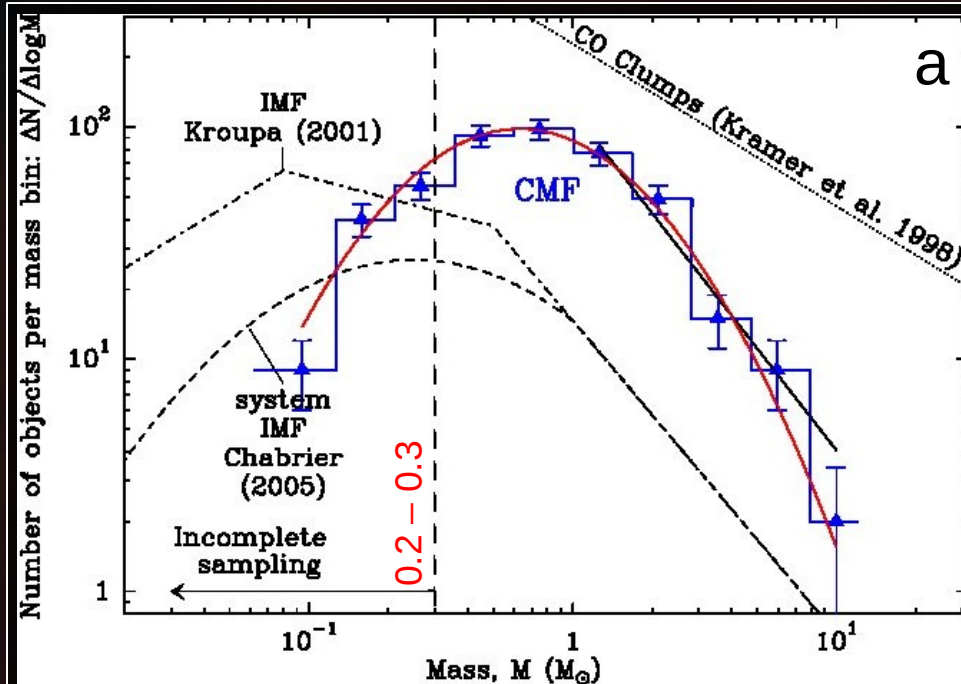
(b) Lognormal fit: peak at $\sim 0.9 M_{\odot}$, standard deviation ~ 0.30 in $\log_{10} M$.

fitted power-law: $dN/d\log M \propto M^{-1.45 \pm 0.2}$

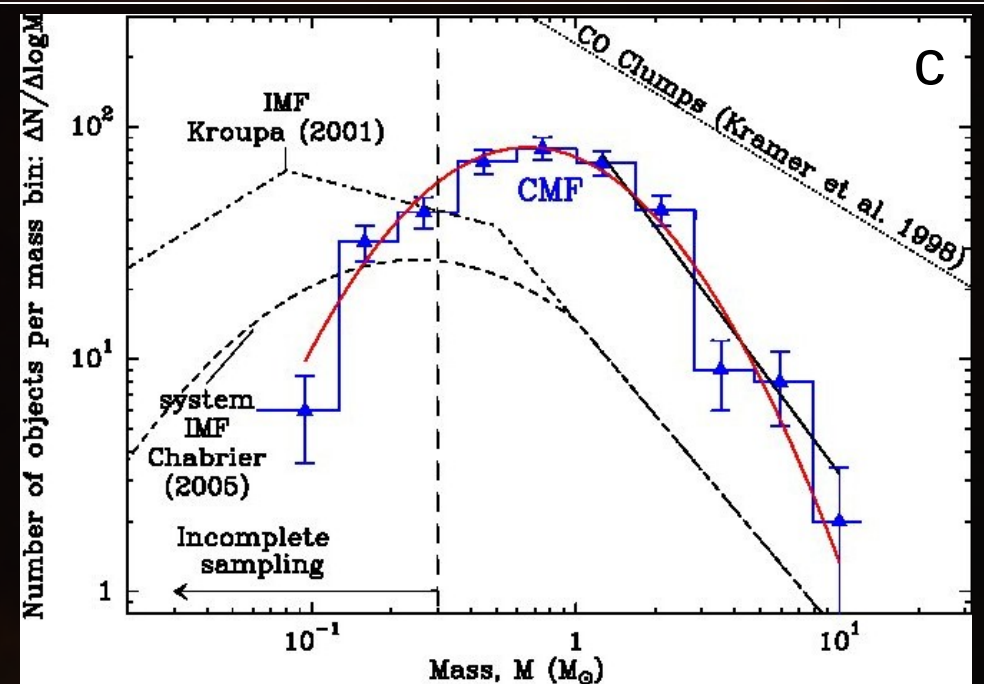
while the **Salpeter IMF** is $dN/d\log M \propto M^{-1.35}$.

PRESTELLAR CORES IN AQUILA

CORE MASS FUNCTIONS II



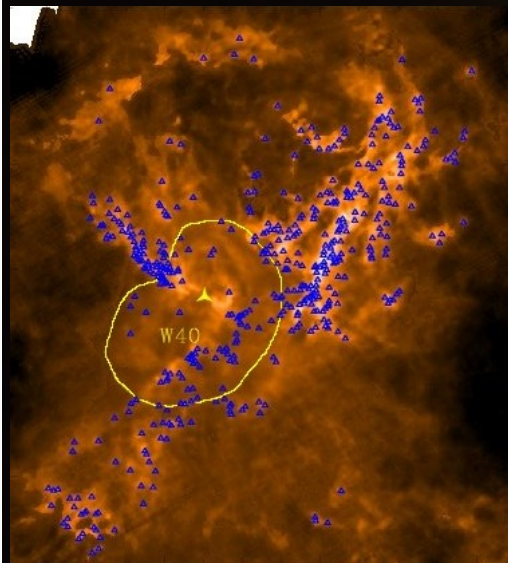
(a) as before



(c) Differential mass function of 368 starless cores, excluding 83 cores toward the PDR region.

(c) Lognormal fit: peak at $\sim 0.7 M_{\odot}$,
 standard deviation ~ 0.40 in $\log_{10} M$.
 fitted power-law: $dN/d\log M \propto M^{-1.5 \pm 0.3}$

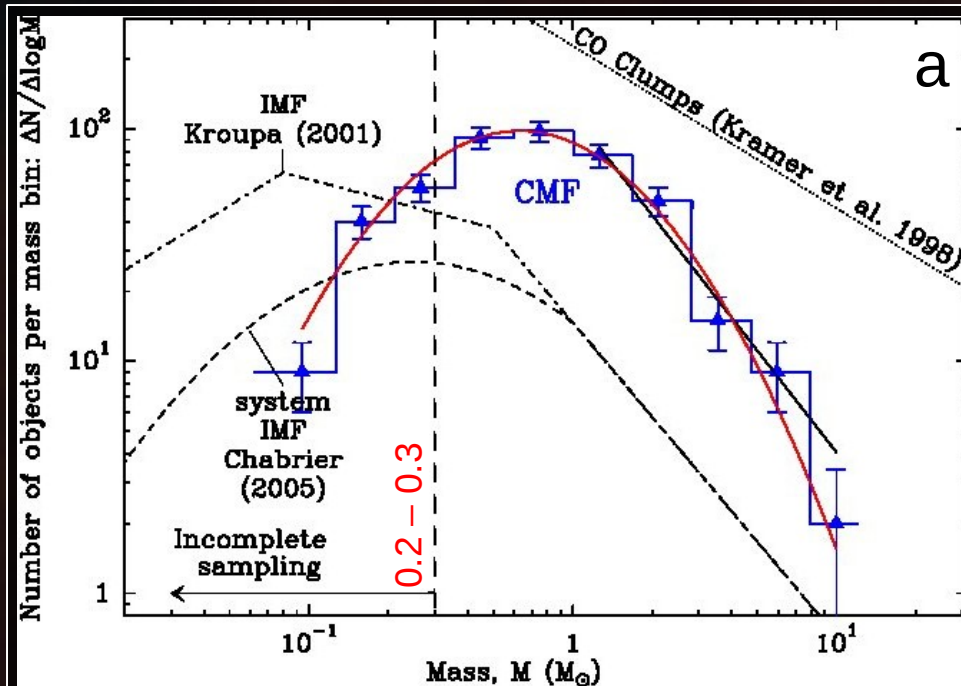
very close to (a), (b), and to the Salpeter
 power-law \Rightarrow robustness of our CMF



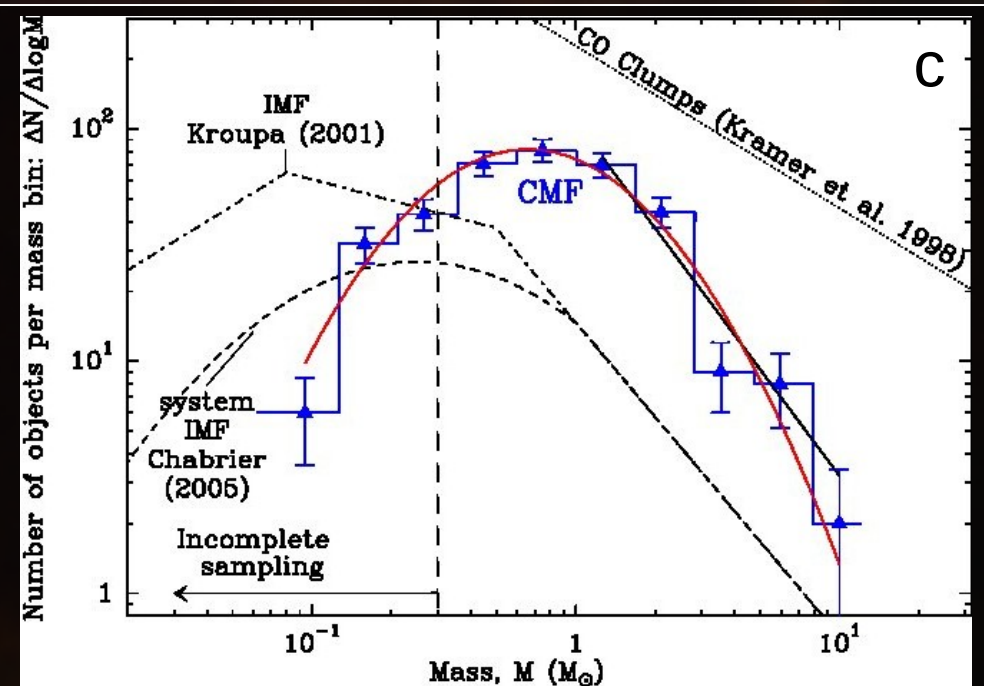
Column density map with starless cores in the Aquila main subfield. The PDR, with high infrared background emission, around the W40 HII region was defined using T_d map (Bontemps et al. 2010).

PRESTELLAR CORES IN AQUILA

CORE MASS FUNCTIONS II



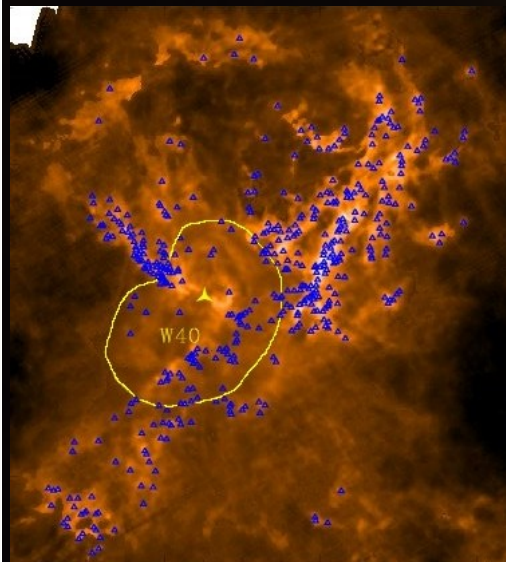
(a) as before



(c) Differential mass function of 368 starless cores, excluding 83 cores toward the PDR region.

(c) Lognormal fit: peak at $\sim 0.7 M_{\odot}$,
 standard deviation ~ 0.40 in $\log_{10} M$.
 fitted power-law: $dN/d\log M \propto M^{-1.5 \pm 0.3}$

very close to (a), (b), and to the Salpeter
 power-law \Rightarrow **robustness of our CMF**

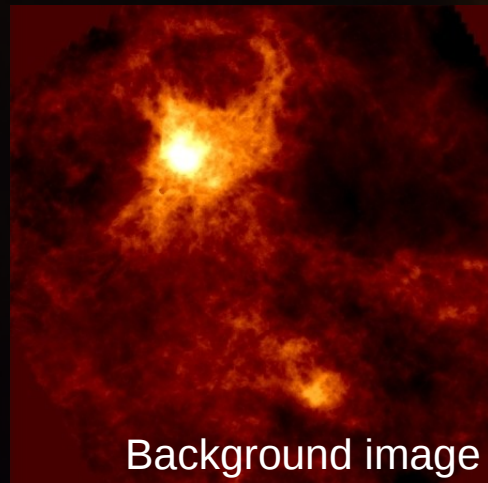


Column density map with starless cores in the Aquila main subfield. The PDR, with high infrared background emission, around the W40 HII region was defined using T_d map (Bontemps et al. 2010).

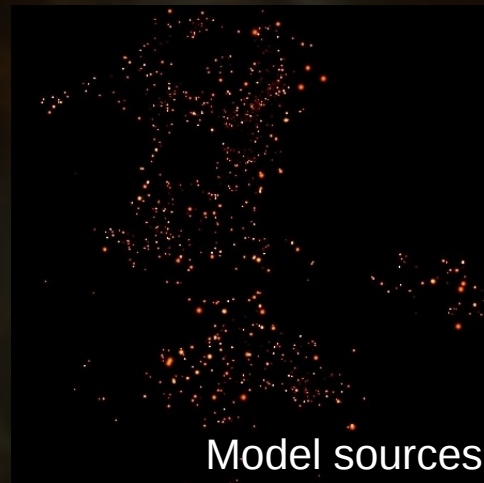


Monte Carlo simulations were performed to estimate the completeness level of our SPIRE/PACS survey, summarized in the following steps:

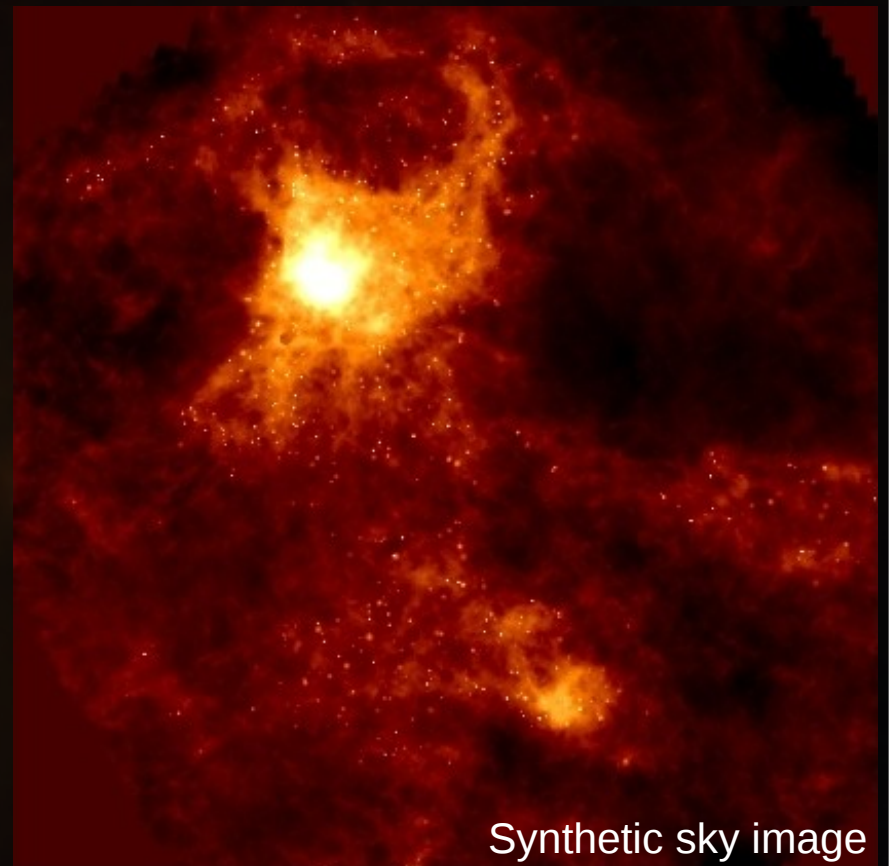
- Subtraction of compact sources (`get sources`) from Herschel maps => **clean maps of background emission**.
- **Radiative transfer simulated objects** (Men'shchikov et al. In prep.): ~ 700 starless cores, ~ 200 protostars with $0.01 - 10 M_{\odot}$, and $M \propto R$ => **inserted at quasi random positions in the clean-background images**.



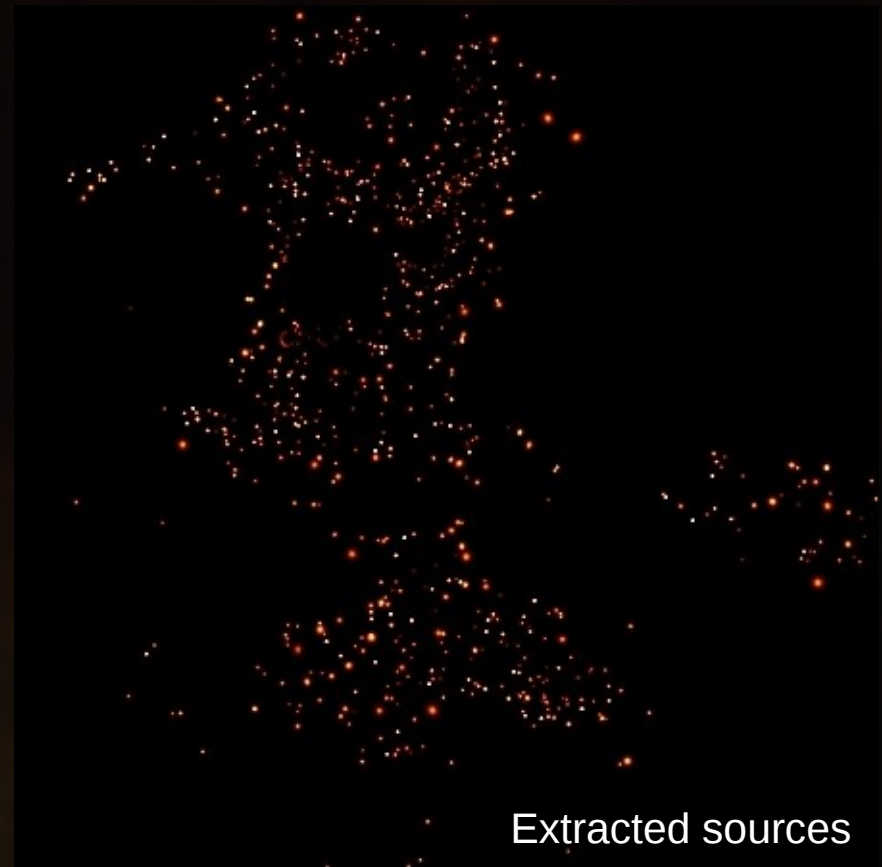
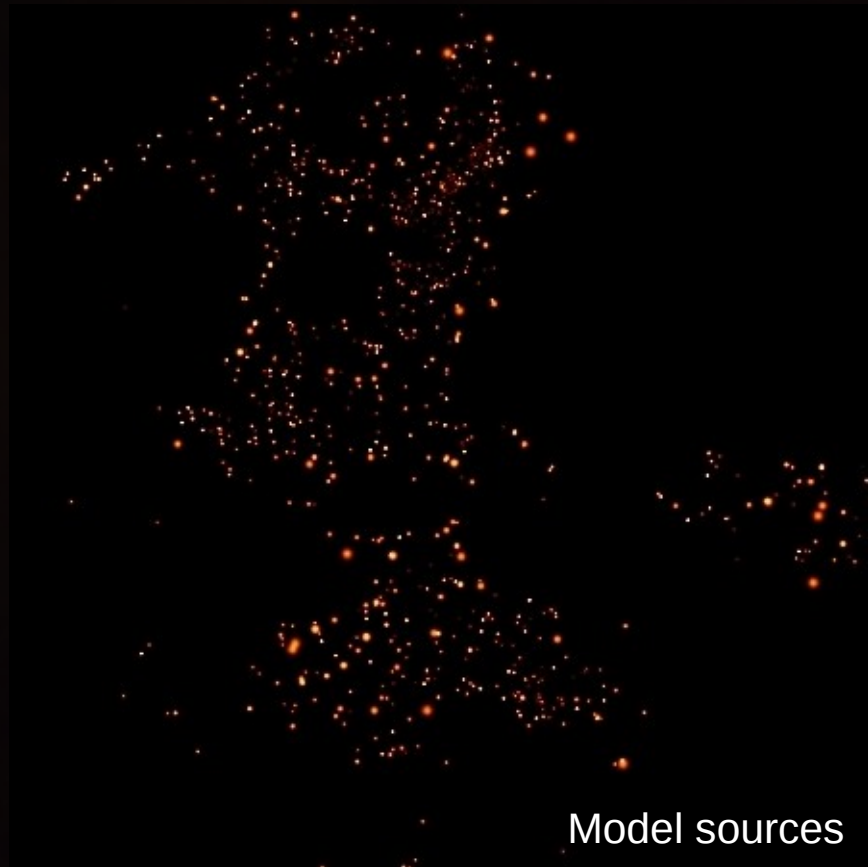
+



=



- **Source extraction** (`get sources`) was performed again **on the synthetic skies**.



Estimated completeness level:

- **for prestellar cores:** 75% and 85% above a core mass of ~ 0.2 and $\sim 0.3 M_{\odot}$
- **for embedded protostars:** $>90\%$ down to $L_{\text{bol}} \sim 0.2 L_{\odot}$

Herschel Gould Belt survey SDP observations of the Aquila Rift complex with SPIRE and PACS at 500 – 70 μm :

- Provided **>500 starless cores in the entire field**, and >400 in the main subfield, **down to $\sim 0.2 - 0.3 M_{\odot}$** .
- **Most of these objects appear to be self-gravitating prestellar cores** that will likely form protostars in the near future.
- **Our results confirm that the shape of the prestellar CMF resembles the stellar IMF**, with much better statistics than earlier sub-millimeter ground-based surveys, and more accurate core masses.
- We conclude that **our mass distributions are robust**, not depending strongly on distance, different sets of extracted sources, and on different locations of the maps.

For more details, see in the A&A Special Issue:

Könyves et al. 2010

André et al. 2010

Bontemps et al. 2010

Men'shchikov et al. 2010

THANK YOU!